

Organic & Biomolecular Chemistry

Accepted Manuscript



This article can be cited before page numbers have been issued, to do this please use: J. Wang, R. Zheng, H. Chen, H. Yao, L. Yan, J. Wei, Z. Lin and Q. Ling, *Org. Biomol. Chem.*, 2017, DOI: 10.1039/C7OB02446K.



This is an Accepted Manuscript, which has been through the Royal Society of Chemistry peer review process and has been accepted for publication.

Accepted Manuscripts are published online shortly after acceptance, before technical editing, formatting and proof reading. Using this free service, authors can make their results available to the community, in citable form, before we publish the edited article. We will replace this Accepted Manuscript with the edited and formatted Advance Article as soon as it is available.

You can find more information about Accepted Manuscripts in the [author guidelines](#).

Please note that technical editing may introduce minor changes to the text and/or graphics, which may alter content. The journal's standard [Terms & Conditions](#) and the ethical guidelines, outlined in our [author and reviewer resource centre](#), still apply. In no event shall the Royal Society of Chemistry be held responsible for any errors or omissions in this Accepted Manuscript or any consequences arising from the use of any information it contains.



Journal Name

ARTICLE

Diarylmaleimide-based branched oligomers: strong full-color emission in both solution and solid film

Jingwei Wang,^a Rong Zheng,^a Huan Chen,^a Huimei Yao,^a Liyu Yan,^b Jie Wei,^b Zhenghuan Lin^{*ab} and Qidan Ling^b

Received 00th January 20xx,
Accepted 00th January 20xx

DOI: 10.1039/x0xx00000x

www.rsc.org/

Maleimide and benzene are employed as dendron and core, respectively, to construct two series of non-conjugate branched oligomers (B3G1 and B1G2) based on diarylmaleimide fluorophores by alkylation reaction. Surface aryl groups are changed to tune the emissive color of branched oligomers from blue (λ_{em} =480 nm) to red (λ_{em} =651 nm), realizing full-color emission. The investigation on the photophysical properties of the oligomers indicates that they display intense emission in both solution and solid film, due to the suppression of intramolecular rotation and intermolecular interaction. Molecular simulation and natural transition orbitals analysis show the electron transition take place in the individual diarylmaleimide for the non-conjugate linkage of fluorophores in branched oligomers. It can avoid the unpredictability of luminescent properties caused by the interaction of fluorophores. In addition, the good solubility, thermostability and oxidative stability of the branched oligomers make them have huge potential in the solution-processable photonic application. These results demonstrate such the design strategy of non-conjugate branched oligomers is a very efficient and constructive method to get high-performance light-emitting materials in both solution and solid film.

Introduction

Organic compounds with strong fluorescence have important applications in the fields of chemosensors^{1,2} and biological probes,^{3,4} photoelectronic devices,⁵⁻⁷ and fluorescent bioimaging.^{8,9} Traditional organic fluorescent compounds with large aromatic system display intense emission in dilute solution, but weak fluorescence in the solid state for long exciton lifetime and aggregation-caused quenching (ACQ) which results from the delocalization of exciton and strong π - π interactions.¹⁰⁻¹² The luminescent process in solution offers a benefit of understanding the emission properties at the molecular levels. However, the ACQ effect badly impedes the practical applications of fluorescent compounds in devices, like organic light-emitting diodes (OLEDs) and organic lasers, etc. Since Tang and his co-workers reported solid-stated fluorescence of siloles and tetraphenylethylenes,^{13,14} a large numbers of organic compounds with aggregation-induced emission (AIE) or aggregation-induced emission enhancement (AIEE) have been developed.¹⁵⁻²² Although AIE- and AIEE-active molecules exhibit intense luminescence in aggregated states, they show non-emission or weak emission in the solution for the non-radiative relaxation of exciton mainly caused by the intramolecular rotation.

Therefore, the dual-state strong emission (DSE) in both solution and solid is significant for a more comprehensive insight of organic luminescence mechanisms and properties, as well as the practical utilization. Just because of this, the DSE-active molecules have received considerable attention in recent years.²³⁻²⁷

In addition, realizing full-color luminescence by regulation of the photophysical properties of organic molecules is a hot topic for wide applications in optoelectronic field.²⁷⁻³¹ Although a combination of several fluorophores with different emitting color, such as blue, green and red, can obtain full-color emission, their different stability and luminescent efficiency would cause a big problem in the practical application. It is important to modify the structure of one fluorophore to achieve tunable emission in both solution and solid. Whereas, the luminescence of organic compound is not as easy to be changed in the solid state as in solution due to the huge effect of packing mode of molecules in solid on the luminescent properties.^{18,32,33} Consequently, it is a big challenge to design new compounds, especially DSE molecules, to realize controllable and tunable fluorescence, even covering the entire visible region.

In this paper, we describe an unprecedented design to construct full-color DSE-active materials by non-conjugately linking a kind of fluorophore into a dendritic structure. The branched structure for DSE molecules design has the following five advantages: (1) The orderly 3D structure can restrain effectively the intermolecular interaction and ACQ for spatial isolation effect, and consequently improve solid-state emission. (2) The bulky dendritic structure can suppress substantially the intramolecular rotation of fluorophore, led to high quantum yield in solution. (3) The branched structure makes the luminescent materials be of good solubility and film-

^a Fujian Key Laboratory of Polymer Materials, Fujian Normal University, Fuzhou 350007, China.

Email: zhlin@fjnu.edu.cn

^b College of Chemistry and Materials Science, Fujian Normal University, Fuzhou 350007, China.

† Electronic supplementary information (ESI) available: Absorption and emission spectra of diarylmaleimide fluorophores, theory calculation data, additional experimental details. See DOI: 10.1039/x0xx00000x

forming ability, which are favorable for solution-processing application. (4) There are many surface groups on the dendritic structure, thus, it is easy to adjust the emitting color of molecules by changing these surface groups. (5) The non-conjugately linkage of dendron can keep the nature of fluorophore unchangeable in the branched molecules. Herein, two series of diarylmaleimide-based branched oligomers (Fig. 1) with different surface groups were designed and synthesized by employing benzene ring as core, and maleimide as branched units. The branched oligomers display intense full-color emission in both solution and solid film.

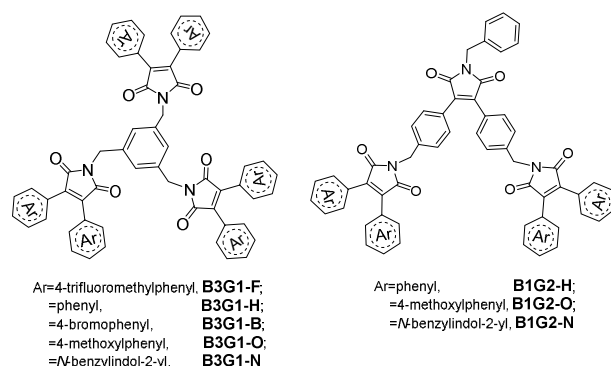


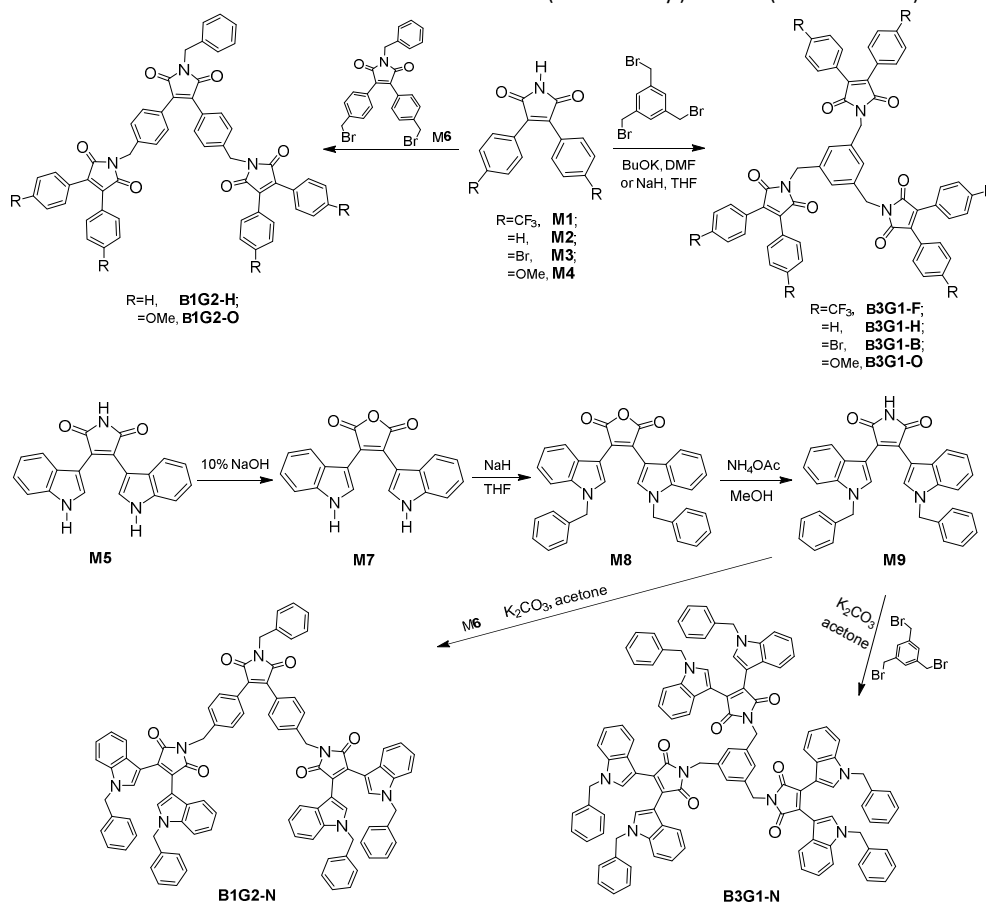
Fig. 1. Structure of B3G1 and B1G2 series dendrimers.

Results and discussion

Design and Synthesis of branched oligomers

3,4-Disubstituted arylmaleimide was chosen as fluorophore to design the branched oligomers for its flexible branched structure, high quantum yield, and tunable emitting color.^{17, 27, 34, 35} These advantages render it be frequently used as a backbone to construct various multifunctional fluorescent materials applied to OLED,^{34, 36-40} anion sensing,^{41, 42} and data storage and process.^{17, 18, 43} Alkylation of maleimide with benzyl bromide is a common reaction employed to synthesize arylmaleimide derivatives in a high yield. Thus, benzene and maleimide were used as core and branched units, respectively, to construct the non-conjugate branched oligomers by alkylation. Different surface aryl groups (trifluoromethylbenzene, benzene, bromobenzene, methoxybenzene and benzylindole) were utilized to adjust the emissive color of branched oligomers (Fig. 1). The branched oligomers include three-branch-core and one-generation ones (B3G1-F, B3G1-H, B3G1-B, B3G1-O and B3G1-N), and one-branch-core and two-generation ones (B1G2-H, B1G2-O and B1G2-N).

Synthetic route of the diarylmaleimide-based branched oligomers is shown in Scheme 1. 3,4-Diphenylmaleimides (M1-M4) were obtained according to a reported procedure.³⁵ B3G1-F, B3G1-H, B3G1-B and B3G1-O were synthesized through a substitution reaction of 3,4-diphenylmaleimides (M1-M4) with 1,3,5-tris(bromomethyl)benzene (core monomer) under strong alkaline



Scheme 1 Synthetic route of branched oligomers.

Journal Name

ARTICLE

condition. The core monomer was replaced by monomer M6 to give B1G2-H and B1G2-O. M6 was obtained by the same synthetic reaction of M1-M4, followed by a substitution reaction of benzylbromide and a bromination of NBS (Scheme S1). The branched oligomers (B3G1-N and B1G2-N) containing diindolylmaleimide fluorophore were prepared from 3,4-diindolylmaleimide (M5) according to a similar synthetic route (Scheme 1). M5 was firstly turned into 3,4-diindolylmaleic anhydride (M7) in 10% NaOH aqueous solution,²⁷ and then converted into monomer M9 through two-step reactions in a high yield. The resulting B3G1-N and B1G2-N could be obtained through the substitution reaction of M9 with M6 and 1,3,5-tris(bromomethyl)benzene, respectively. It was found keeping the reaction in the dark place was favorable to the synthesis of B3G1 and B1G2, due to the instability of core monomer. For the same reason, the reaction have to be run in the temperature below 100 °C, which, however, results in low yield of trisubstitued products (resulted molecules). Additionally, the synthesis of B3G1 and B1G2 with different surface aryl groups should choose different alkali/solvent system. Otherwise, the resulted branched molecules could not be obtained. For example, strong base NaH was needed in the synthesis of B3G1-F with benzene as surface groups, while the combination of weak base K₂CO₃ and polar solvent acetone was suitable for the synthesis of B3G1-N and B1G2-N with indole as surface groups. The branched oligomers are soluble in common solvents, such as toluene, dichloromethane, chloroform, THF, DMF, etc.

Photophysical properties in solution

Photophysical properties of the branched oligomers in chloroform (10 μM) were investigated first. Fig. 2 gives their absorption and emission spectra which are compared with the spectra of the corresponding arylmaleimide monomers (M1-M5) in Fig. S1. Due to the non-conjugated linkage between fluorophores (arylmaleimides), branched oligomers display similar optic properties as their corresponding monomers. There are mainly two absorption bands between 250 nm and 600 nm in the absorption spectra of branched oligomers (Fig. 2a). The first band before 325 nm is assigned to the π - π^* transition of separating maleimide or aryl units, while the second band after 325 nm should be derived from the π - π^* transition involving both maleimide and aryl moieties. For B3G1-O, B3G1-N, B1G2-O and B1G2-N, the second band companied by a shoulder peak shows a red shift in solution. For example, maximum absorption peak bathochromically shifts from 360 nm of B3G1-F to 482 nm of B3G1-N in chloroform. The red shift should be ascribed to the strong electron-pushing ability of the surface aryl groups, methoxylbenzene and indole, which cause an intramolecular charge transition (ICT) from the aryl groups to maleimide.

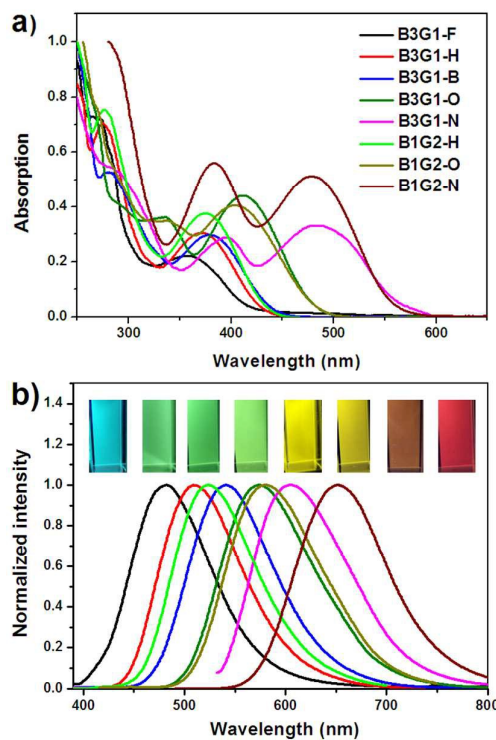


Fig. 2 Absorption (a) and emission (b) spectra of oligomers in CHCl₃ solution, and their photographs (inset in b) taken under 365 nm UV light. Branched oligomers in b arranged from left to right: B3G1-F, B3G1-H, B1G2-H, B3G1-B, B3G1-O, B1G2-O, B3G1-N, and B1G2-N.

The effect of the peripheral aryl groups on emission of branched oligomers is more significant than on their absorption. From the emission spectra of branched oligomers shown in Fig. 2b, it was found that they display substantial red shift with the increasing electron-pushing ability of the aryl groups, resulting in a full-color emission overlapping from blue of B3G1-F to red region of B1G2-N. Relative to M2, M4 and M5, B1G2 type branched oligomers show larger red-shift than B3G1 type ones (Fig. S2). It should be ascribed to the space distribution of three fluorophores. Three arylmaleimide equally disperse around the benzene core, while they concentrate on one side of the core, which makes the environmental polarity of fluorophore in B1G2 is larger than in B3G1. To confirm the polar effect on the luminescent properties of arylmaleimide fluorophores, their emission spectra in different solvent were investigated (Fig. S3). These fluorophores indeed show a red-shift of the emission band with the increasing polarity of solvents. Experimental data of the photophysical properties of branched oligomers and monomers are summarized in Table 1 and Table S1, respectively.

Journal Name

ARTICLE

Table 1 Experimental data of photophysical properties of branched oligomers

	λ_{obs} (nm)	λ_{emr} (nm)	Φ_f (%)	τ (ns)	k_r^b (ns ⁻¹)	k_{nr}^c (ns ⁻¹)
	S / F ^a	S / F	S / F	S / F	S / F	S / F
B3G1-F	360 / 369	482 / 481	42 / 65	10.34 / 10.64	0.041 / 0.061	0.056 / 0.033
B3G1-H	362 / 368	508 / 507	86 / 54	17.97 / 10.84	0.048 / 0.050	0.008 / 0.042
B3G1-B	379 / 383	541 / 541	64 / 65	13.91 / 3.70	0.046 / 0.176	0.026 / 0.095
B3G1-O	412 / 421	574 / 571	63 / 60	12.11 / 5.76	0.052 / 0.104	0.031 / 0.069
B3G1-N	482 / 488	605 / 606	24 / 28	7.19 / 2.74	0.033 / 0.102	0.106 / 0.263
B1G2-H	376 / 377	524 / 518	67 / 66	16.18 / 8.41	0.041 / 0.078	0.020 / 0.043
B1G2-O	404 / 414	580 / 575	37 / 35	12.75 / 6.77	0.029 / 0.052	0.049 / 0.096
B1G2-N	479 / 483	651 / 640	20 / 10	6.23 / 2.46	0.032 / 0.041	0.128 / 0.366

^a S = Chloroform solution, F = Film. ^b Radiative rate constant $k_r = \Phi_f/\tau$. ^c Non-radiative rate constant $k_{nr} = (1-\Phi_f)/\tau$.

For the rigid structure, all of branched oligomers show higher quantum yield (Φ_f) than their corresponding arylmaleimide monomers in solution. For example, Φ_f of B3G1-F and B3G1-N is the double of their corresponding arylmaleimide fluorophores (M1 and M5). The fluorescent lifetimes (τ) of branched oligomers were measured using time-resolved single photon counting technique and determined to be in the range of 6.23-17.97 ns in solution. However, the branched oligomers with same fluorophore, such as B3G1-H and B1G2-H, B3G1-O and B1G2-O, B3G1-N and B1G2-N, display similar lifetime in solution. It indicates that the photophysical properties of branched oligomers are closely related to the arylmaleimide fluorophores. Time-resolved transient luminescence decay of branched oligomers in dilute solution is plotted in Fig. S4. Consequently, their radiative rate constant (k_r) and non-radiative rate constant (k_{nr}) can be estimated from the formula $k_r = \Phi_f/\tau$ and $k_{nr} = (1-\Phi_f)/\tau$, respectively (Table 1). High radiative rate constant of branched oligomers results in their high quantum yield.

Theory calculation

Above experimental results suggest that each arylmaleimide in branched oligomers behaves as an isolated fluorophore with little electronic interaction between dendrons. To get insight into the photophysical properties of these arylmaleimides and branched oligomers, including their ground-state and excited-state properties, density functional theory (DFT) and time-dependent DFT (TD-DFT) calculations were performed by using B3LYP and cam-6-31G (d) as function and basis set, respectively. DFT-optimized geometry of the five arylmaleimides (M1-M5) has a non-planar conformation with the twist angle between the maleimide ring and aryl ring at 22-46° (Fig. S5). The computed vertical absorption properties from TD-DFT given in Table S2 indicate that the first excited-state (S_1) transition occurs predominantly between HOMO and LUMO. The computed

electron density distribution of molecular orbitals of the arylmaleimides is depicted in Fig. S6. The HOMO are mainly populated on two symmetrically equivalent aryl rings, while the LUMO is concentrated on the central maleimide moiety. Localization degree of electrons is more significant with the increase of electron-pushing ability of aryl group. This is an indication of a charge transfer (CT) character for the maximum absorption band which is sensitive to the environmental polarity. It is in agreement with the experimental result in the solution.

DFT-optimized geometry of branched molecules in ground state reveals that each fluorophore keeps similar twisted conformation as their corresponding arylmaleimide monomers (Fig. S7). The twisted fluorophores linked by a methylene group make branched oligomers present a screwier structure which is helpful to eliminate the intermolecular interplay when aggregated in the condensed phase. TD-DFT calculated results of the first 6 singlet excited states of branched oligomers are given in Table S3-S10. The calculated vertical absorption transition energy (S_1) has much better agreement with the experimental ones with an overestimation less than 0.18 eV (Table 2). It was found that all of branched oligomers have degenerate excited states (S_1 and S_2 for B1G2-O and B1G2-N, S_1 , S_2 and S_3 for other branched oligomers) due to same separated fluorophores. It is difficult to visualize the location excitons and possible electronic interactions within the branched oligomers for the presence of such degenerate states and multiple orbital transitions for each electronic transition. Consequently, natural transition orbitals (NTOs) method was used to give a qualitative description of an electronic excitation. From NTO pairs for the first three excited singlet states of branched oligomers (Fig. 3, S8-S13), note that all of electronic transition of degenerate states takes place in the occupied and virtual orbitals of individual fluorophore, corresponding to their HOMO and LUMO orbitals (Fig. S6). It indicates that there is no electronic communication between

arylmaleimide fluorophores in branched oligomers, which makes isolated fluorophore. branched oligomers behave similar photophysical properties as

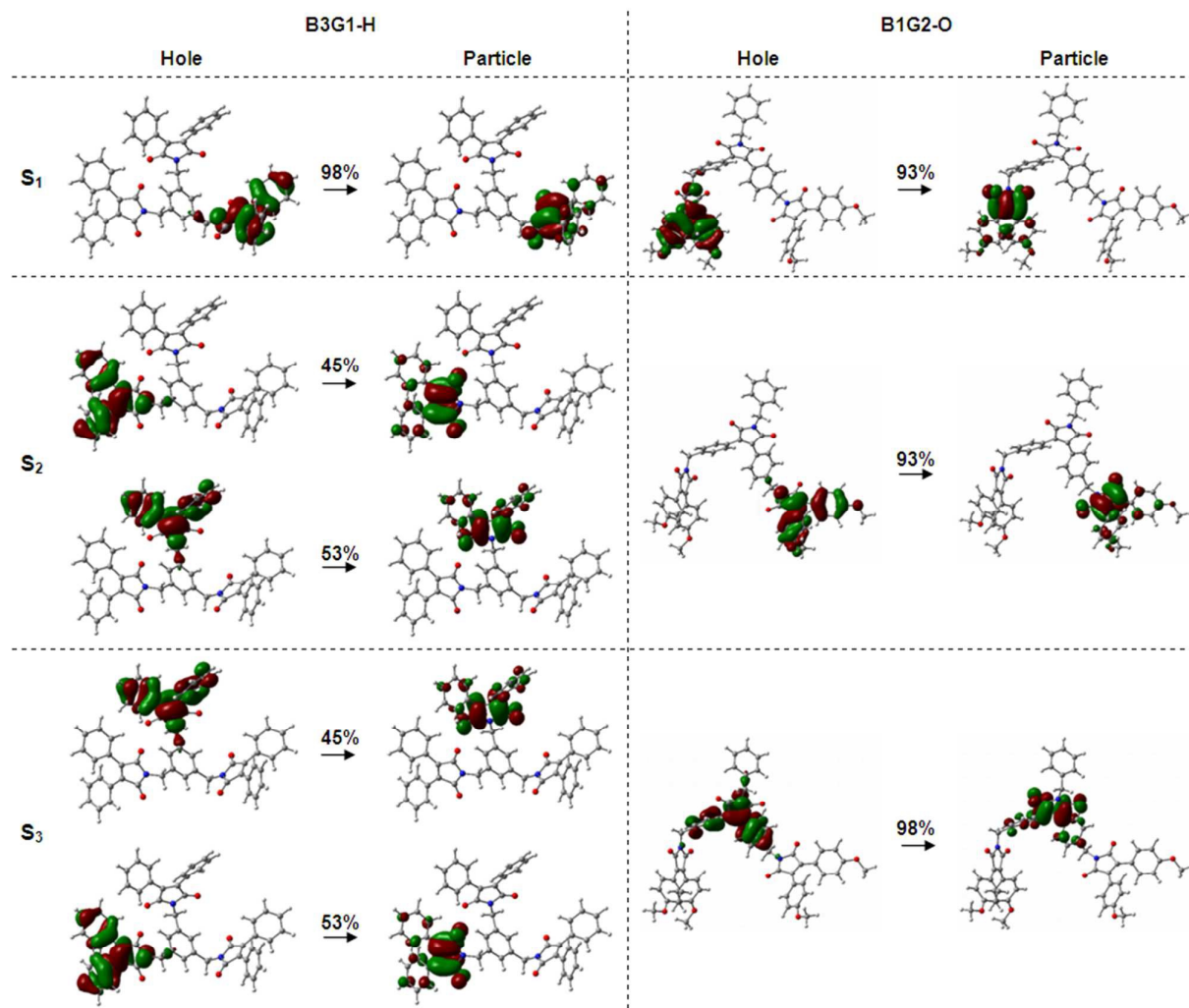


Fig. 3 Natural transition orbital pairs for the first three excited singlet states of B3G1-H and B1G2-O.

Table 2 Experimental absorption transition energies (E) and Calculated absorption photophysics with electronic excitation energies (E) and oscillator strength (f) of arylmaleimides

	Exptl E , eV	Calcd E , eV (f)		
		S_1	S_2	S_3
B3G1-F	3.44	3.52 (0.17)	3.55 (0.28)	3.57 (0.10)
B3G1-H	3.44	3.45 (0.14)	3.47 (0.23)	3.49 (0.11)
B3G1-B	3.27	3.36 (0.22)	3.39 (0.33)	3.41 (0.16)
B3G1-O	3.01	3.16 (0.20)	3.17 (0.32)	3.20 (0.19)
B3G1-N	2.57	2.75 (0.15)	2.77 (0.24)	2.88 (0.17)
B1G2-H	3.30	3.40 (0.21)	3.43 (0.09)	3.43 (0.25)
B1G2-O	3.07	3.13 (0.16)	3.13 (0.28)	3.38 (0.26)
B1G2-N	2.59	2.67 (0.24)	2.69 (0.15)	3.34 (0.18)

Photophysical properties in films

Photophysical properties of the branched oligomers in solid film were investigated next. The films were obtained by spin-coating their chloroform solution (10 mg/mL) at the speed of 1000 r/s. The absorption and emission spectra of branched oligomers are shown in Fig. S14 and Fig. 4a, respectively. For a comparison, the spectra properties of monomers (M1-M5) in solid were determined and shown in Fig. S15, as well as the relevant data summarized in Table S1. As mentioned above, the absorption and emission spectra of dendimers in solution exhibit similar characteristic as that of their corresponding monomers, due to the non-conjugated linkage between diarylmaleimides in branched oligomers. However, the discrepancy of absorption wavelength (λ_{abs}) of branched oligomers between solution and films is obviously smaller than that of monomers, resulted from the specific dendric structure that can effectively inhibit the intermolecular interaction. For instance, the maximum λ_{abs} of M2 bathochromically shift 22 nm from 361 nm in solution to 383 nm in films. The red-shift was found to be 6 nm for

ARTICLE

Journal Name

B3G1-H, and 1 ns for B1G2-H. The same situation was found in the emission spectra of branched oligomers in solid film. For instance, the difference of maximum λ_{em} between solution and solid is more than 10 nm for M1, M3 and M5, but less than 3 nm for B3G1-F, B3G1-B and B3G1-N. Like in solution, branched oligomers in solid film exhibit full-color emission ranging from blue (481 nm) to red (640 nm).

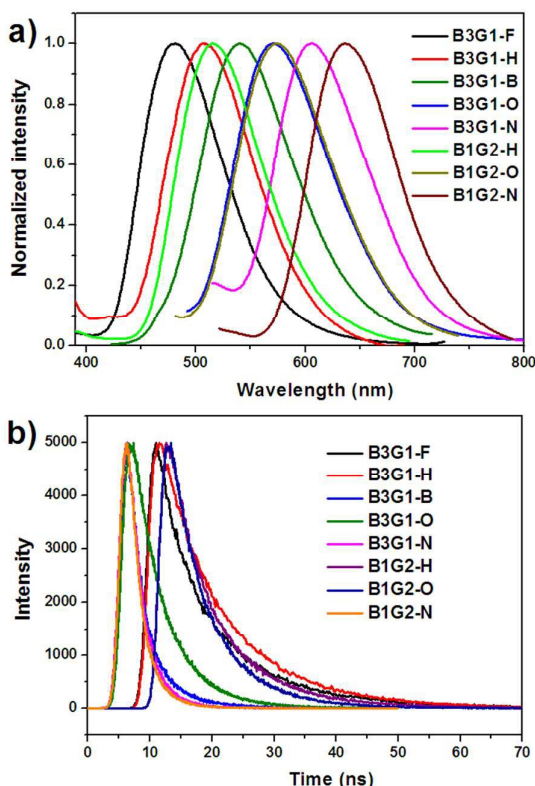


Fig. 4 Emission (a) spectra and transient fluorescence decays (b) of branched oligomers in solid film.

Although the spectra properties of branched oligomers mainly depend on optic transition of the individual arylmaleimide fluorophores, their quantum yield very differs from the corresponding monomers. For the weak intermolecular interaction, branched oligomers in films show high emission efficiency and radiative rate constant. Φ_f of branched oligomers in solid film matches that in solution. Especially for B3G1-F, B3G1-B and B3G1-N, their Φ_f in film exceeds that in solution. It was found that the Φ_f of most of the monomers in solid is lower than that in solution for strong intermolecular interactions, such as π - π stacking and dipole-dipole interaction. In particular, M5 shows strong ACQ feature. In the case of branched oligomers, the separation and protection of fluorophores in dendric structure make them be of high emission efficiency in both solution and solids. Time-resolved transient luminescence decay of branched oligomers in solid film is plotted in Fig. 4b. After fitting the curves, their fluorescent lifetime was found to ranges from 2.46 ns to 10.84 ns, which is smaller than in solution. B3G1-H, B3G1-O and B3G1-N show similar lifetime as B1G2-H, B1G2-O and B1G2-N, respectively, for the same fluorophore.

Thermal and electrochemical properties

Thermal properties of polymers were investigated by thermogravimetric analysis (TGA) under a nitrogen atmosphere at a scan speed of 10 °C/min. From the TGA plots shown in Fig. 5, it can be found that most of branched oligomers exhibit excellent thermal properties with the decomposed temperature (T_d) above 400 °C, except for B3G1-O. However, the 5% weight-loss temperature ($T_{5\%}$) of B3G1-O, B3G1-N, B1G2-O and B1G2-N was found at 277 °C, 282 °C, 212 °C and 272 °C, respectively (Table S11), which is lower than that of other branched oligomers. It should be related to the deprivation of peripheral methoxy or benzyl groups in B3G1-O, B1G2-O, B3G1-N and B1G2-N in high temperature. In general, the thermal stability of the branched oligomers is good enough to meet their application need for devices.

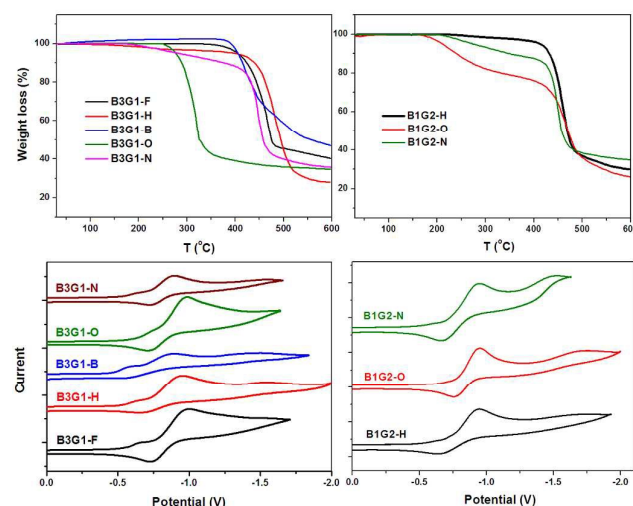


Fig. 5 TGA curves (upper) of branched oligomers and their CV curves (bottom) in solid film.

Electrochemical properties of the branched oligomers were measured by cyclic voltammetry (CV) at a scan rate of 100 mV/s in a 0.1 M n-Bu₄NPF₆ solution in acetonitrile with Ag/AgCl as reference electrode. The CV data and reduction curves of branched oligomers are given in Table S11 and Fig. 5, respectively. All of branched oligomers demonstrate mostly reversible reduction scan with similar reduction wave at about -0.70 V for their common electron-deficient unit, maleimide ring. The recorded CV curves were calibrated using a ferrocene/ferrocenium (Fc/Fc⁺) redox couple (4.8 eV below the vacuum level) as an external standard. The $E_{1/2}$ of the Fc/Fc⁺ redox couple was found to be 0.40 V vs the Ag quasireference electrode. As a result, the LUMO and HOMO energy levels of the branched oligomers can be estimated using the empirical equation $E_{LUMO} = -(E_{red}^{onset} + 4.40)$ eV and $E_{HOMO} = E_{LUMO} - E_g^{opt}$, where E_{red}^{onset} and E_g^{opt} stand for the onset potentials of reduction and optical band gap, respectively. The LUMO levels of the branched oligomers lie around -3.70 eV, while their HOMO levels locate in the range of -5.90 ~ -6.69 eV for the different electron-pushing groups in the fluorophore (Fig. 6). The fact that all of branched oligomers have oxidation potentials larger than 5.9 eV

suggests their stability at ambient conditions. These results will guide the application of the oligomers in photoelectric devices.

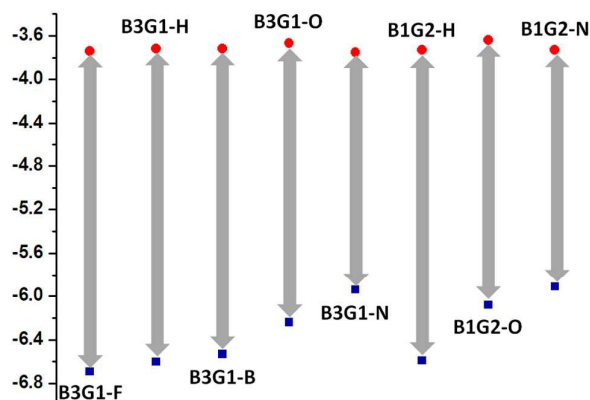


Fig. 6 HOMO and LUMO energy levels for branched oligomers in solid film.

Experimental

Materials and Measurements

All the reagents and solvents used in the experiments were obtained from commercial suppliers and used as received without further purification, unless otherwise noted. Thin layer chromatography was performed on G254 silica gel plates of Qingdao Haiyang Chemical. Column chromatography was conducted on Yantai Huanghai brand silica gel (200-300 mesh). Diarylmalimides M1, M2, M3, M4 and M7 were synthesized according to a previously reported method.^{27,35}

Low temperature reaction was performed on a Yuhua DFY-5/80 reactive bath. High-resolution MALDI-TOF mass spectra were recorded on a Bruker microflex LRF spectrometer. NMR spectra were measured in *d*-CDCl₃ or *d*-DMSO on a Bruker Ascend 400 FT-NMR spectrometer. ¹H and ¹³C chemical shifts were quoted relative to the internal standard tetramethylsilane. UV-vis spectra were obtained on a Shimadzu UV-2600 spectrophotometer. The PL spectra were probed on a Shimadzu RF-5301PC fluorescence spectrophotometer. Fluorescence lifetime and absolute quantum yield values of solution and solid were measured using an Edinburgh Instruments FLS920 Fluorescence Spectrometer with a 6-inch integrating sphere. Thermo gravimetric analysis (TGA) was measured by a Mettler 851e with a heating rate of 10 °C min⁻¹ under flowing nitrogen. Cyclic voltammetry (CV) was performed on a CHI600D electro-chemical analyzer in anhydrous THF containing tetra-*n*-butyl-ammonium hexafluorophosphate (TBAPF6, 0.1 M) as supporting electrolyte at 298 K. A conventional three electrode cell was used with a platinum working electrode and a platinum wire as the counter electrode. The Pt working electrode was routinely polished with a polishing alumina suspension and rinsed with acetone before use. The measured potentials were recorded with respect to Ag/AgCl reference electrode. All electrochemical measurements were carried out under atmospheric pressure of nitrogen.

Molecular Simulations

Theory calculations were carried out with the Gaussian 09 program. Geometry at ground state was optimized with the density functional theory (DFT) using the B3LYP functional and 6-31G* basis set. The vertical excited energies were calculated with the time-dependent density functional theory (TD-DFT) at CAM-B3LYP/6-31G*.

Synthesis of compound M9

3,4-Bis(indolyl)maleic anhydride (M7) (800 mg, 2.4 mmol) was mixed with NaH (168 mg, 7 mmol) in dried THF (23 ml) under a nitrogen atmosphere, and the solution was stirred at 0 °C for 45 minutes. To the mixture was added benzyl bromide (1.2 mL, 10 mmol), the reaction mixture was kept stirring at reflux under argon for 10 h, and cooled to room temperature. The reaction was diluted with ethyl acetate and successively washed with 1 M dilute hydrochloric acid, water and brine. It was then dehydrated over anhydrous MgSO₄ and dried in vacuo to give the crude product of 3,4-bis-(*N*-benzylindolyl) maleic anhydride (M8) which was used without further purification.

3,4-Bis-(*N*-benzylindolyl) maleic anhydride (600 mg, 1.18 mmol), anhydrous ammonium acetate (2.270 mg, 29.5 mmol) and anhydrous methanol (60 mL) was added to hydrothermal synthesis reactor. The reaction was allowed to put into an oven at 100 °C overnight, and cooled to room temperature. The reaction was extracted with ethyl acetate. The organic phase was washed with brine. It was then dehydrated over anhydrous MgSO₄. After removing the solvent, the crude product was purified by column chromatography with ethyl acetate/petroleum ether (1:4) as the eluant, affording compound M9 in 95% yield. ¹H NMR (400 MHz, CDCl₃) δ 7.73 (d, *J* = 3.4 Hz, 2H), 7.58 (s, 1H), 7.37–7.27 (m, 6H), 7.21 (d, *J* = 8.3 Hz, 2H), 7.15–7.09 (m, 4H), 7.03 (d, *J* = 20.4, 13.2, 4.5 Hz, 4H), 6.76–6.71 (m, 2H), 5.35 (s, 4H). ¹³C NMR (100 MHz, DMSO) δ 173.25, 138.11, 136.25, 132.68, 129.03, 128.10, 127.90, 127.31, 126.66, 122.32, 121.53, 120.04, 111.04, 105.80, 49.85.

Synthesis of compound B3G1-F

M1 (517 mg, 1.35 mmol) and NaH (39 mg, 1.62 mmol) were placed in a 25 mL flask. 8 mL of dry THF was injected into flask under a nitrogen atmosphere at 0 °C and was vigorously stirred for 40 min. Then, 1,3,5-tris(bromomethyl)benzene (80 mg, 0.224 mmol) in dry THF (2 mL) was added to the reaction mixture, which was heated to reflux for 12 h. After the reaction mixture was cooled to room temperature, it was added 1M dilute hydrochloric acid and extracted with ethyl acetate. The organic phase was washed with brine, and then dehydrated over anhydrous MgSO₄. After removing the solvent, the crude product was purified by column chromatography with DCM /petroleum ether (1:2) as the eluant, affording light blue solids of B3G1-F. Yield: 41%. ¹H NMR (400 MHz, CDCl₃) δ 7.58 (d, *J* = 8.3 Hz, 13H), 7.52 (d, *J* = 8.2 Hz, 11H), 7.45 (s, 3H), 4.82 (s, 6H). ¹³C NMR (100 MHz, CDCl₃) δ 169.37, 137.23, 136.34, 132.31, 131.98, 131.42, 130.24, 128.28, 125.70, 41.85. MALDI MASS *m/z* [M+Na+H]⁺ calcd 1293.2058, found 1293.6165.

Synthesis of compound B3G1-H

ARTICLE

Journal Name

M2 (0.8 g, 3.2 mmol), 1,3,5-tris(bromomethyl)benzene (141 mg, 0.4 mmol) and potassium tert-butyrate (2.17 g, 19.2 mmol) were placed in a 10 mL flask. 6 mL of dry DMF was injected into flask under a nitrogen atmosphere at 90 °C and was vigorously stirred for 24 h. After the reaction mixture was cooled to room temperature, the reaction was extracted with ethyl acetate. The organic phase was washed with brine. It was then dehydrated over anhydrous MgSO₄. After removing the solvent, the crude product was purified by column chromatography with DCM/petroleum ether (1:2) as the eluant, affording green solids of compound B3G1-H. Yield: 48%. ¹H NMR (400 MHz, CDCl₃) δ 7.36 (d, J = 8.0 Hz, 13H), 7.27 (t, J = 7.3 Hz, 7H), 7.24 – 7.17 (m, 13H), 4.72 (s, 6H). ¹³C NMR (100 MHz, CDCl₃) δ 169.50, 136.63, 135.49, 129.12, 128.88, 127.81, 127.64, 127.27, 40.80. MALDI MASS m/z [M+Na+H]⁺ calcd 885.2815, found 885.0221.

Synthesis of compound B3G1-B

M3 (1 g, 2.47 mmol), 1,3,5-tris(bromomethyl)benzene (150 mg, 0.42 mmol) were placed in a 50 mL flask. 5 mL of dry DMF was injected into flask under a nitrogen atmosphere. Then, a fresh sodium methoxide solution made from sodium (87 mg, 3.8 mmol) and methanol (15 mL) was added to the reaction mixture at 0 °C and vigorously stirred for 40 min, which was heated to 100 °C for 12 h. After the reaction mixture was cooled to room temperature and added 1 M HCl aqueous solution, it was extracted with ethyl acetate. The organic phase was washed with brine, and then dehydrated over anhydrous MgSO₄. After removing the solvent, the crude product was purified by column chromatography with DCM/petroleum ether (1:5) as the eluant, affording green solids of compound B3G1-B. Yield: 37%. ¹H NMR (400 MHz, DMSO) δ 7.61 – 7.55 (m, 12H), 7.27 (dd, J = 10.0, 8.1 Hz, 15H), 4.72 (s, 6H). ¹³C NMR (100 MHz, CDCl₃) δ 169.72, 137.29, 135.42, 132.04, 131.33, 128.12, 127.09, 124.87, 41.68. MALDI MASS m/z [M+K]⁺ calcd 1373.7045, found 1373.1160.

Synthesis of compound B3G1-O

M4 (507 mg, 1.64 mmol) and NaH (45 mg, 1.968 mmol) were placed in a 25 mL flask. 8 mL of dry THF was injected into flask under a nitrogen atmosphere at 0 °C and was vigorously stirred for 40 min. Then, 1,3,5-tris(bromomethyl)benzene (60 mg, 0.164 mmol) in dry THF (2 mL) was added to the reaction mixture, which was heated to reflux for 12 h. After the reaction mixture was cooled to room temperature and added 1 M HCl aqueous solution, it was extracted with ethyl acetate. The organic phase was washed with brine, and then dehydrated over anhydrous MgSO₄. After removing the solvent, the crude product was purified by column chromatography with DCM/petroleum ether (3:1) as the eluant, affording yellow solids of compound B3G1-F. Yield: 38%. ¹H NMR (400 MHz, CDCl₃) δ 7.37 (t, J = 8.5 Hz, 12H), 7.32 (s, 3H), 6.73 (d, J = 8.8 Hz, 12H), 4.68 (s, 6H), 3.75 (s, 18H). ¹³C NMR (100 MHz, CDCl₃) δ 170.82, 160.60, 137.53, 134.21, 131.51, 127.84, 121.40, 113.99, 55.24, 41.48. MALDI MASS m/z [M+H]⁺ calcd 1042.3551, found 1041.9077.

Synthesis of compound B3G1-N

M9 (317 mg, 0.624 mmol), 1,3,5-tris(bromomethyl)benzene (35 mg, 0.098 mmol) and potassium carbonate (129 mg, 0.936 mmol) were placed in a 25 mL flask. 6 mL of acetone was injected into flask under nitrogen atmosphere and was vigorously stirred for 12 h at 90 °C. After the reaction mixture was cooled to room temperature. The reaction mixture was extracted with ethyl acetate, and washed with brine. It was then dehydrated over anhydrous MgSO₄. After removing the solvent, the crude product was purified by column chromatography with ethyl acetate/petroleum ether (1:4) as the eluant, affording red solids of compound B3G1-N. Yield: 48%. ¹H NMR (400 MHz, DMSO) δ 7.93 (s, 6H), 7.28 (tt, J = 14.1, 7.7 Hz, 27H), 7.13 (d, J = 7.1 Hz, 12H), 6.93 (t, J = 7.7 Hz, 6H), 6.84 (d, J = 8.0 Hz, 6H), 6.53 (t, J = 7.6 Hz, 6H), 5.36 (s, 12H), 4.77 (s, 6H). ¹³C NMR (100 MHz, DMSO) δ 171.68, 138.63, 137.88, 136.24, 132.99, 129.00, 127.90, 127.33, 126.49, 126.18, 122.39, 121.72, 120.17, 111.09, 105.71, 49.85, 41.61. MALDI MASS m/z [M+H]⁺ calcd 1637.6422, found 1638.1194.

Synthesis of compound B1G2-H and B1G2-O

M2 or M4 (1.14 mmol) and NaH (32 mg, 1.33 mmol) were placed in a 25 mL flask. 6 mL of dry THF was injected into flask under a nitrogen atmosphere at 0 °C and was vigorously stirred for 40 min. Then, M6 (100 mg, 0.19 mmol) in dry THF (2 mL) was added to the reaction mixture, which was heated to reflux for 12 h. After the reaction mixture was cooled to room temperature and added 1 M HCl aqueous solution, it was extracted with ethyl acetate. The organic phase was washed with brine. It was then dehydrated over anhydrous MgSO₄. After removing the solvent, the crude product was purified by column chromatography with ethyl acetate/petroleum ether (1:4) as the eluant, affording green or yellow solids of compound B1G2-H or B1G2-O.

B1G2-H. Green solids. Yield: 36%. ¹H NMR (400 MHz, CDCl₃) δ 7.53 – 7.28 (m, 33H), 4.80 (d, J = 7.8 Hz, 6H). ¹³C NMR (100 MHz, CDCl₃) δ 170.37, 138.22, 136.35, 136.28, 135.76, 130.55, 130.22, 129.91, 128.96, 128.86, 128.77, 128.70, 128.58, 128.53, 128.10, 127.89, 42.05, 41.65. MALDI MASS m/z [M+Na+H]⁺ calcd 885.2815, found 885.2761.

B1G2-O. Green solids. Yield: 33%. ¹H NMR (400 MHz, CDCl₃) δ 7.49 – 7.20 (m, 22H), 6.79 (d, J = 8.7 Hz, 7H), 4.70 (s, 6H), 3.75 (s, 12H). ¹³C NMR (100 MHz, CDCl₃) δ 170.90, 170.36, 160.76, 138.42, 136.38, 135.74, 134.14, 131.47, 130.92, 130.18, 128.88, 128.69, 128.00, 127.87, 121.24, 114.11, 55.31, 42.04, 41.49. MALDI MASS m/z [M+Na+H]⁺ calcd 1005.3237, found 1005.2536.

Synthesis of compound B1G2-N

M9 (510 mg, 1 mmol), M6 (106 mg, 0.2 mmol) and potassium carbonate (207 mg, 1.5 mmol) were placed in a 25 mL flask. 8 mL of dry acetone was injected into flask under a nitrogen atmosphere and was vigorously stirred for 12 h at reflux. After the reaction mixture was cooled to room temperature, it was extracted with ethyl acetate. The organic phase was washed with brine. It was then dehydrated over anhydrous MgSO₄. After removing the solvent, the crude product was purified by plate chromatography with ethyl acetate/petroleum ether (1:4) as the eluant, affording red solids of compound B1G2-N. Yield: 31%. ¹H NMR (400 MHz, CDCl₃) δ 7.72 (s, 4H), 7.42 (s, 10H), 7.27 (dd, J = 13.8, 6.7 Hz, 15H), 7.19 (d, J = 8.2 Hz,

4H), 7.10 (d, $J = 7.1$ Hz, 8H), 7.01 (dd, $J = 17.1, 8.0$ Hz, 8H), 6.72 (t, $J = 7.5$ Hz, 4H), 5.36 – 5.22 (m, 8H), 4.83 (d, $J = 19.1$ Hz, 4H), 4.75 (s, 2H). ^{13}C NMR (100 MHz, CDCl_3) δ 171.93, 170.40, 138.85, 136.59, 136.44, 136.36, 135.75, 132.07, 130.17, 128.86, 128.73, 128.67, 127.86, 127.09, 126.83, 126.44, 122.42, 122.28, 120.20, 109.99, 106.42, 50.57, 41.99, 41.50. MALDI MASS m/z $[\text{M}+\text{Na}]^+$ calcd 1041.5084, found 1041.8810.

Conclusions

An effective design method was presented to construct highly efficient fluorescent materials in both solution and solid film, by non-conjugately linking fluorophores into the branched oligomers. According to the method, two series of branched oligomers, including three-branch-core and one-generation ones (B3G1-F, B3G1-H, B3G1-B, B3G1-O and B3G1-N), and one-branch-core and two-generation ones (B1G2-H, B1G2-O and B1G2-N), were synthesized by employing diarylmaleimide as fluorophore. Surface aryl groups were changed to tune the luminescent color of branched oligomers. In order of electron-pushing ability, they are trifluoromethylbenzene (B3G1-F), benzene (B3G1-H and B1G2-H), bromobenzene (B3G1-B), methoxybenzene (B3G1-O and B1G2-O) and benzylindole (B3G1-N and B1G2-N). The emissive wavelength of branched oligomers bathochromically shift from 480 nm of B3G1-F to 651 nm of B1G2-N with the increasing electron-pushing ability of surface groups. Theory calculation shows that the optic properties of branched oligomers basically depend on the electronic transition of individual fluorophore. There are no interactions between the fluorophores in branched oligomers for their non-conjugated structure. However, the emissive intensity of branched oligomers in both solution and solid film has been greatly improved, relative to arylmaleimide fluorophores. The good solubility, chemical stability, and thermostability of the branched oligomers make them have huge potential in the solution-processable photonic application.

Conflicts of interest

There are no conflicts of interest to declare.

Acknowledgements

This work was supported by the National Natural Science Foundation of China (21374017, 21401023 and 21574021), the Natural Science Foundation of Fujian Province (2017J01684), and Educational Commission of Fujian Province (JA14068).

Notes and references

- 1 L. He, B. Dong, Y. Liu and W. Lin, *Chem. Soc. Rev.*, 2016, **45**, 6449-6461.
- 2 Y. Zhou, J. F. Zhang and J. Yoon, *Chem. Rev.*, 2014, **114**, 5511-5571.
- 3 E. I. Galanzha, R. Weingold, D. A. Nedosekin, M. Sarimollaoglu, J. Nolan, W. Harrington, A. S. Kuchyanov, R. G. Parkhomenko, F. Watanabe and Z. Nima, *Nat. Commun.*, 2017, **8**, 15528.

- 4 J. Xu, J. Pan, X. Jiang, C. Qin, L. Zeng, H. Zhang and J. F. Zhang, *Biosens. Bioelectron.*, 2016, **77**, 725-732.
- 5 A. J. C. Kuehne and M. C. Gather, *Chem. Rev.*, 2016, **116**, 12823-12864.
- 6 M. Y. Wong and E. Zysman-Colman, *Adv. Mater.*, 2017, **29**, 1605444.
- 7 Z. Yang, Z. Mao, Z. Xie, Y. Zhang, S. Liu, J. Zhao, J. Xu, Z. Chi and M. P. Aldred, *Chem. Soc. Rev.*, 2017, **46**, 915-1016.
- 8 J.-T. Hou, W. X. Ren, K. Li, J. Seo, A. Sharma, X.-Q. Yu and J. S. Kim, *Chem. Soc. Rev.*, 2017, **46**, 2076-2090.
- 9 P. Reineck and B. C. Gibson, *Adv. Opt. Mater.*, 2017, **5**, 1-26.
- 10 Y.-X. Li, M.-P. Pang, Z.-W. Zhang, G.-B. Li and G.-X. Sun, *RSC Adv.*, 2013, **3**, 14950-14953.
- 11 X. L. Xu, F. W. Lin, W. Xu, J. Wu and Z. K. Xu, *Chem. Eur. J.*, 2015, **21**, 984-987.
- 12 L. Zong, Y. Xie, C. Wang, J.-R. Li, Q. Li and Z. Li, *Chem. Commun.*, 2016, **52**, 11496-11499.
- 13 Y. Dong, J. W. Y. Lam, A. Qin, J. Liu, Z. Li and B. Z. Tang, *Appl. Phys. Lett.*, 2007, **91**, 011111.
- 14 J. Luo, Z. Xie, J. W. Lam, L. Cheng, H. Chen, C. Qiu, H. S. Kwok, X. Zhan, Y. Liu and D. Zhu, *Chem. Commun.*, 2001, 1740-1741.
- 15 Y. Liu, Y. Lei, F. Li, J. Chen, M. Liu, X. Huang, W. Gao, H. Wu, J. Ding and Y. Cheng, *J. Mater. Chem. C*, 2016, **4**, 2862-2870.
- 16 P. Mazumdar, D. Das, G. P. Sahoo, G. Salgado-Morán and A. Misra, *Phys. Chem. Chem. Phys.*, 2015, **17**, 3343-3354.
- 17 X. Mei, K. Wei, G. Wen, Z. Liu, Z. Lin, Z. Zhou, L. Huang, E. Yang and Q. Ling, *Dyes Pigm.*, 2016, **133**, 345-353.
- 18 X. Mei, G. Wen, J. Wang, H. Yao, Y. Zhao, Z. Lin and Q. Ling, *J. Mater. Chem. C*, 2015, **3**, 7267-7271.
- 19 X. Wang, Y. Wu, Q. Liu, Z. Li, H. Yan, C. Ji, J. Duan and Z. Liu, *Chem. Commun.*, 2015, **51**, 784-787.
- 20 Z. Xie, C. Chen, S. Xu, J. Li, Y. Zhang, S. Liu, J. Xu and Z. Chi, *Angew. Chem. Int. Ed.*, 2015, **54**, 7181-7184.
- 21 B. Xu, J. He, Y. Mu, Q. Zhu, S. Wu, Y. Wang, Y. Zhang, C. Jin, C. Lo and Z. Chi, *Chem. Sci.*, 2015, **6**, 3236-3241.
- 22 S. Xu, T. Liu, Y. Mu, Y. F. Wang, Z. Chi, C. C. Lo, S. Liu, Y. Zhang, A. Lien and J. Xu, *Angew. Chem. Int. Ed.*, 2015, **54**, 874-878.
- 23 A. S. Abd-El-Aziz, C. Agatemor, N. Etkin and B. Wagner, *Macromol. Rapid Commun.*, 2016, **37**, 1235-1241.
- 24 G. Chen, W. Li, T. Zhou, Q. Peng, D. Zhai, H. Li, W. Z. Yuan, Y. Zhang and B. Z. Tang, *Adv. Mater.*, 2015, **27**, 4496-4501.
- 25 M. Huang, R. Yu, K. Xu, S. Ye, S. Kuang, X. Zhu and Y. Wan, *Chem. Sci.*, 2016, **7**, 4485-4491.
- 26 M. Li, Y. Niu, X. Zhu, Q. Peng, H.-Y. Lu, A. Xia and C.-F. Chen, *Chem. Commun.*, 2014, **50**, 2993-2995.
- 27 X. Mei, J. Wang, Z. Zhou, S. Wu, L. Huang, Z. Lin and Q. Ling, *J. Mater. Chem. C*, 2017, **5**, 2135-2141.
- 28 H. Chen, Y. Tang, H. Shang, X. Kong, R. Guo and W. Lin, *J. Mater. Chem. B*, 2017, **5**, 2436-2444.
- 29 J. Han, J. You, X. Li, P. Duan and M. Liu, *Adv. Mater.*, 2017, **29**, 1606503.
- 30 H. Tachibana, N. Aizawa, Y. Hidaka and T. Yasuda, *Acs Photonics*, 2017, **4**, 223-227.
- 31 X. Wei, L. Bu, X. Li, H. Agren and Y. Xie, *Dyes Pigm.*, 2017, **136**, 480-487.
- 32 Z. Lin, X. Mei, E. Yang, X. Li, H. Yao, G. Wen, C.-T. Chien, T. J. Chow and Q. Ling, *CrystEngComm*, 2014, **16**, 11018-11026.
- 33 K. Wang, H. Zhang, S. Chen, G. Yang, J. Zhang, W. Tian, Z. Su and Y. Wang, *Adv. Mater.*, 2014, **26**, 6168-6173.
- 34 Z. Lin, Y.-D. Lin, C.-Y. Wu, P.-T. Chow, C.-H. Sun and T. J. Chow, *Macromolecules*, 2010, **43**, 5925-5931.
- 35 H. C. Yeh, W. C. Wu and C. T. Chen, *Chem. Commun.*, 2003, 404-405.

ARTICLE

Journal Name

- 36 Z. Lin, Y.-S. Wen and T. J. Chow, *J. Mater. Chem.*, 2009, **19**, 5141-5148.
- 37 J. Wang, Y. Zhao, K. Wei, G. Wen, X. Li, Z. Lin and Q. Ling, *Synth. Met.*, 2017, **230**, 18-26.
- 38 K. Wei, G. Wen, Y. Zhao, Z. Lin, X. Mei, L. Huang and Q. Ling, *J. Mater. Chem. C*, 2016, **4**, 9804-9812.
- 39 Y. Zhao, Z. Lin, Z. Zhou, H. Yao, W. Lv, H. Zhen and Q. Ling, *Org. Electron.*, 2016, **31**, 183-190.
- 40 Y. Zhao, H. Yao, K. Wei, H. Zhen, E. Yang, Z. Lin and Q. Ling, *Phys. Chem. Chem. Phys.*, 2017, **19**, 12642-12646.
- 41 Z. Lin, Y. Ma, X. Zheng, L. Huang, E. Yang, C.-Y. Wu, T. J. Chow and Q. Ling, *Dyes Pigm.*, 2015, **113**, 129-137.
- 42 H. Yao, J. Wang, H. Chen, X. Mei, Z. Su, J. Wu, Z. Lin and Q. Ling, *RSC Adv.*, 2017, **7**, 12161-12169.
- 43 R. Zheng, X. Mei, Z. Lin, Y. Zhao, H. Yao, W. Lv and Q. Ling, *J. Mater. Chem. C*, 2015, **3**, 10242-10248.